BY ERIC R. BACHMANN, XIAOPING YUN, AND ANNE BRUMFIELD

Limitations of Attitude Estimation Algorithms for Inertial/Magnetic Sensor Modules

Real-time tracking of the orientation or attitude of rigid bodies has wide applications in robotics [1], helicopters [2], teleoperation, augmented reality, and virtual reality [3]. Limb segment orientation can be estimated through the attachment of an inertial/magnetic sensor module to each segment as depicted in Figure 1. Given the length of each of the segments, their estimated orientation based on sensor module data, and their arrangement relative to one another, the posture of the body can be determined. This method of orientation and posture estimation is desirable since it is not dependent on any artificially generated reference signal and does not suffer from any line of sight restrictions [4].

Inertial/magnetic sensor modules and their associated data filtering algorithms are designed to be capable of estimating three degrees of orientation over a wide area in a variety of unprepared tracking environments. The sensor modules commonly contain three linear accelerometers and three magnetometers. The accelerometers are orthogonally mounted in a triad as are the magnetometers. Sensor modules designed for more dynamic applications may also contain three orthogonally mounted angular rate sensors for use as a high-frequency data source. Each of the triads is mounted such that there is an individual sensor aligned with one of the principle axes of the coordinate frame of the sensor module. Thus, the total number of sensors contained in modules designed to provide data for estimating orientation in dynamic applications is commonly nine.

In orientation estimation algorithms designed to process inertial/magnetic sensor data, accelerometers are used to measure the gravity vector relative to the coordinate frame of the sensor module. Accelerometers allow accurate determination of pitch and roll but cannot be used to sense rotations about the gravity or vertical axis. Magnetometers are thus commonly used to measure azimuth or rotation in the horizontal plane relative to a "fixed" reference. The data from the incorporated sensors is normally fused using a Kalman or complementary filtering algorithm. Foxlin et al.

Investigating the Effects of Magnetic Variations on Inertial/Magnetic Orientation Sensors

Digital Object Identifier 10.1109/M-RA.2007.901320

1070-9932/07/$25.00©2007 IEEE

describe two commercial sensor modules containing accelerometers, magnetometers, and angular rate sensors designed for head tracking applications [5], [6]. Sensor fusion is performed using a complementary separate-bias Kalman filter. Bachman et al. propose a quaternion-based complementary filter for human body tracking [3], [7]. The filter is able to track through all orientations without singularities and continuously correct for bias and drift errors associated with low-cost angular rate sensors without a need for stationary periods. Gallagher et al. present a simpler complementary filter algorithm with lower computational complexity in [8]. Luinge describes a Kalman filter designed for human body tracking applications in [9]. The primary difference between the work presented in this article and that of Luinge is that Luinge does not use magnetometers. In the absence of magnetometers, drift about the vertical axis is reduced by limiting body segment orientation using a kinematic human body model. The kinematic model incorporates biomechanical constraints on the joints. This method allows calculation of accurate relative orientation between adjacent segments. The proposed Kalman filter is useful for long periods of measurement if only inclination is required. In [10], Zhu and Zhou describe a linear Kalman filter algorithm designed to smooth accelerometer and magnetometer readings. Rather than estimating individual limb segment orientations relative to a fixed reference frame, the system determines joint angles in axis/angle form using data from the two sensor modules mounted on the two segments adjacent to the joint. Kraft describes an unscented, quaternion-based Kalman filter for real-time estimation of a rigid body orientation [11]. Simulation results demonstrate the general validity of the described filter. Yan and Yuan describe a single-frame orientation tracking algorithm that uses low-cost sensor modules to take two axis measurements of gravity and the local magnetic field [12]. Elevation, roll, and azimuth angles are sequentially calculated and the method is limited to orientation tracking within a hemisphere. In [13], Gebre-Egziabher et al. describe another single-frame attitude determination algorithm for aircraft applications. The algorithm is based on the QUEST (Quaternion ESTimator) algorithm [14], which was originally designed to determine spacecraft attitude given a set of three-dimensional (3-D) reference vectors and their corresponding observation or measurement vectors. In the case of [13], the local magnetic field and gravity vectors are used as reference vectors.

In the above studies, with the exception of the work by Luinge [9], both the gravity and local magnetic field vectors are treated as fixed references. In the case of the gravity vector, the assumption that it is fixed leads to no difficulties since this vector does in fact point straight down in any inertial frame located on or near the surface of the earth. Making the same assumption regarding the local magnetic field vector can, however, lead to problems. In a typical room setting, the direction as well as the magnitude of the local magnetic field vector can be expected to vary due to the presence of ferrous objects or electrical appliances. Relative weighting can be used to reduce the weight applied to magnetometer data in comparison to other sensor information. However, slow drift about the vertical axis in the presence of a sustained change in the direction of the magnetic field vector will still occur. Reducing the weight given to magnetic data does, however, make it possible to reduce orientation errors resulting from transients in the local magnetic field. Such weighting techniques allowing manual adjustment of magnetometer gains are described in [3], [5], and [8].

This article describes several experiments designed to examine small-scale magnetic interference caused by typical objects and how this interference can be expected to affect the accuracy of orientation estimates produced using data from inertial/magnetic sensor modules. The results provide insight into the limitations of inertial/magnetic sensor module orientation tracking. They indicate that while errors due to local variations in a common room environment caused by individual objects can be significant, in most cases they can be avoided by maintaining a separation of approximately 1 m from the

Figure 1. *Prototype body tracking system based on inertial/magnetic sensor modules.*

Magnetic permeability is a constant of proportionality that exists between magnetic induction and magnetic field intensity that can be viewed as a measure of how easily magnetic lines of flux will pass through a given material.

source of interference. The interference caused by combined sources in a noisy indoor environment can, however, be quite complex. The results also indicate that inertial/magnetic sensor modules can be used to track link orientation of a mechanical arm relative to an Earth-fixed reference frame.

Background

The following paragraphs go deeper into the theory of orientation estimation algorithms designed for inertial/magnetic sensor modules and briefly describe three types of sensor modules. Specifically, the modules discussed are the InterSense InertiaCube, the MicroStrain 3DM-G, and the MARG III. The MARG III was designed by the authors and manufactured by McKinney Technology. Basic background on the ambient magnetic field of the Earth and how it is distorted by ferrous objects and electrically powered devices is then provided. Methods of calibrating magnetic field variations are then discussed.

Inertial/Magnetic Sensor Modules

Inertial/magnetic sensor modules have be been fabricated by both industry and university research laboratories. Filtering algorithms designed for these sensor modules are based on inertial and magnetic quantities directly related to the motion and orientation of a sensor module. Algorithms designed for use with inertial/magnetic sensor modules produce accurate orientation estimates by taking advantage of the complementary nature of the sensed quantities in order to determine orientation.

For a static or slow-moving rigid body, accelerometer triad output can normally be averaged (or low pass filtered) for a short period of time in order to measure the components of the gravity vector in the sensor coordinate frame. Determination of the relationship of the measurement in the sensor coordinate frame to the gravity vector in the Earth coordinate frame allows estimation of orientation relative to the horizontal plane. However, in the event that the sensor module is rotated about the vertical axis, the projection of the gravity vector on each of the principle axes of the accelerometer will not change. Since the accelerometer triad cannot be used to sense a rotation about the vertical axis, an orthogonally mounted triad of magnetometers is commonly used to measure the local magnetic field vector in body coordinates and allow determination of orientation relative to the vertical. Thus, combining magnetometer data with accelerometer data provides a complete method for estimating the orientation.

Alternatively, assuming the initial orientation of the body is known, integration of the output of a triad of orthogonally mounted angular rate sensors provides another method of estimating orientation. If the rate sensors are susceptible to noise or bias effects, as is the case for the small low-cost sensors used in inertial/magnetic sensor modules, these estimates become useless after a short period. To avoid lag or overshoot in dynamic applications, many inertial/magnetic sensor filtering algorithms combine high-frequency angular rate sensor data with low-frequency accelerometer and magnetometer data in a complementary manner to produce continuously accurate orientation estimates in real-time.

Based on the work of Foxlin, InterSense Inc. developed and marketed a sensor module called the InertiaCube2. The primary application for this module is head tracking. Manufacturer's literature indicates that the InertiaCube2 is capable of measuring angular rates, linear accelerations, and the local magnetic field along three axes. Dimensions for the InertiaCube2 are 29 mm × 24 mm × 34 mm. Orientation estimates are made by a proprietary extended Kalman filter [5], [6]. Manufacturer's literature lists an accuracy of 1.0° and an update rate of 180 Hz.

The Microstrain 3DM-G Gyro Enhanced Orientation Sensor also contains a triad of orthogonally mounted angular rate sensors, a triad of orthogonally mounted accelerometers, and a triad of orthogonally mounted magnetometers. Sensor data are processed by a proprietary filtering algorithm running on an embedded microcontroller. Manufacturer's literature lists an accuracy of ±5° for arbitrary orientations. Unlike the InertiaCube2, unscaled as well as scaled raw data output are available from this unit. The update rate is 76.6 Hz. Unit dimensions are 65 mm × 90 mm × 25 mm.

The MARG III sensor module shown in Figure 2 is a research prototype developed by the Modeling, Virtual Environments and Simulation (MOVES) Institute at the Naval Postgraduate School [15]. Primary sensing components for this unit include Tokin CG-L43 ceramic rate gyros, Analog Devices ADXL202E micromachined accelerometers, and Honeywell HMC1051Z and HMC1052 one and two-axis magnetometers. The MARG III sensor module incorporates a Texas Instruments MSP430F149 ultra-low-power, 16-bit RISC architecture microcontroller. Overall, dimensions are approximately 18 mm × 30 mm × 25 mm. The sensor module includes a magnetic set/reset circuit to cancel magnetometer temperature drift and avoid magnetic saturation effects. Various complementary and Kalman filters based on a quaternion representation of orientation have been used to process MARG III sensor data [3], [16]. Estimation accuracy has been measured to be better than 1°.

Magnetic Field Variations

Magnetic fields surround permanent magnets or electrical conductors. They can be visualized as a collection of magnetic

flux lines. Flux lines are said to emanate from a "north" pole and return to a "south" pole in a magnet. Flux density, or magnetic induction, is a measure of the number of flux lines passing through a given cross sectional area. Magnetic field strength is a measure of force produced by an electric current or a permanent magnet. Magnetic field strength decreases with the cube of the distance from the source. While magnetic field strength and magnetic flux density are not the same, they are equal within a vacuum. Magnetic permeability is a constant of proportionality that exists between magnetic induction and magnetic field intensity. It can be viewed as a measure of how easily magnetic lines of flux will pass through a given material. In the presence of an object made of a material with a relatively high permeability, magnetic field lines will bend toward or be attracted to the object. Thus, distortion can be expected to occur near large ferrous objects [17].

The direction and magnitude of ambient magnetic field at a given point is the vector sum of all magnetic fields present at that point. The dominate field in most cases is that of the Earth, which varies from approximately 0.23 to 0.61 Gauss. However, additional magnetic fields caused by conductors through which a current is flowing and magnets also contribute to the total field at a given position. All contributing fields will be distorted by objects made of materials with a high magnetic permeability.

In an indoor environment, sources of magnetic interference are constantly present and can include common items such as computer monitors, fluorescent lighting, and powered-up electrical wiring inside walls. Table 1 lists the fields generated by some common appliances. In some cases the strength of the generated field exceeds that of the Earth within a short distance of the appliance. If a magnetic sensor is placed in this nearby area the generated field can be expected to have an effect on the direction and magnitude of the field measured by the sensor. Unless the field generated by the appliance happens to be aligned with that of the Earth, the reported direction will not be that of the Earth's magnetic field. In a room-size environment such fields would constitute local variations from the average field in the room. It is variations of this type and their effect on the orientation estimates produced by inertial magnetic sensors with which this article is concerned.

Magnetic Field Calibration

Magnetic distortions caused by ferrous objects that have a fixed location and orientation relative to the magnetometers being used to determine the direction of the local magnetic field vector can be separated into two categories. These categories are hard iron and soft iron effects. Hard iron objects are permanently magnetized. Soft iron objects are unmagnetized unless under the influence of a magnetic field.

Hard iron effects add a constant offset to the vector measured by magnetometers making up an orthogonal triad. They can be compensated for in the horizontal plane by rotating the magnetometers together with the involved hard iron objects and sampling at enough points in a circle to determine the offset relative to the horizontal plane. Determination of all components of the offset requires rotation in more than one plane. Unlike hard iron effects, soft iron effects do not produce a constant offset. Soft iron influences are dependent on orientation [19]. Thus, correcting for soft iron effects often requires the construction of a heading dependent lookup table [20]. Construction of a 3-D lookup table is difficult and time consuming. Thus, in a strap-down navigation system, magnetic readings are usually projected onto the horizontal plane using a tilt sensor before corrections are made.

In general, calibration is best approached by removing any soft iron materials and dealing with hard iron effects directly. The magnetic properties of many materials are actually in between those of soft and hard iron and change over time. During a calibration performed at any given time, the effects of such subpermanent materials will appear to be permanent like hard iron. However, since the effects observed are not truly permanent, calibration procedures must be repeated on a periodic basis [17].

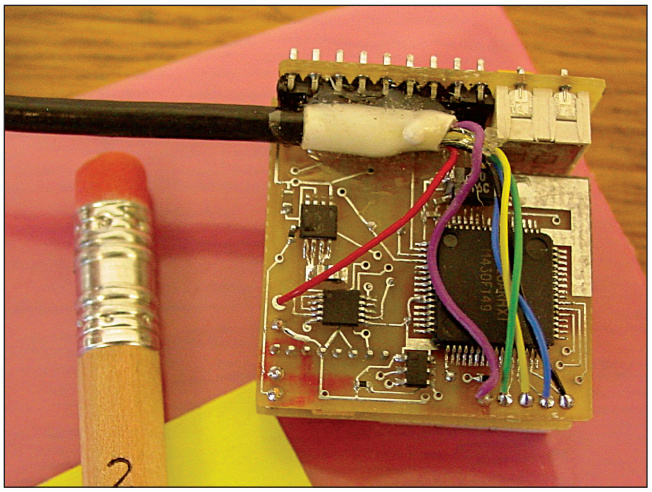

Figure 2. *MARG III inertial/magnetic sensor module.*

Table 1. Common magnetic field magnitudes in Gauss at 15 and 30 cm (adapted from [18]).

	Distance (15 cm) Field (Gauss)	Distance (30 cm) Field (Gauss)
Can Opener	1.60	0.27
Electric Saw	1.20	0.25
Vacuum Cleaner	0.75	0.20
Electric Shaver	0.65	0.10
Mixer	0.61	0.11
Hair Dryer	0.50	0.07
Electric Drill	0.20	0.03
Portable Heater	0.15	0.04
Fluorescent Light Fixture	0.13	0.04
Fan (Range Hood)	0.09	0.03
Television	0.07	0.02

In an indoor environment, sources of magnetic interference are constantly present and can include common items such as computer monitors, fluorescent lighting, and powered-up electrical wiring inside walls.

It should be emphasized that the above discussion of calibration focuses only on effects caused by objects that have a fixed position and orientation relative to a magnetic sensor. In a tracking application, moving inertial/magnetic sensor modules can be expected to constantly change position and orientation relative to ferrous objects and other sources of magnetic distortion. These magnetic distortions will not only change from position to position but can also be expected to change over time as the configuration of the tracking area itself changes. The nature of these distortions and their possible effects on orientation estimation algorithms designed for inertial/magnetic sensor modules is the primary focus of this article.

An Experimental Investigation

Inertial/magnetic sensor module filtering algorithms are dependent on sensing the local magnetic field to eliminate drift in the azimuth portion of orientation estimates. Given that variations in the direction and magnitude of the ambient magnetic field can be expected to occur as a result of the presence of ferrous materials and electrical appliances operating in the tracking environment, what type of estimation errors can be expected and how large can the estimation errors be expected to be? Knowing the answer to this question provides insight into when inertial/magnetic sensor modules can be expected to work properly with minimal estimation error and what type of algorithm modifications could be expected to improve performance. The experiments described below attempt to answer this question. In the first series of experiments, several types of sensor modules are subjected to controlled changes in the direction and strength of the sensed magnetic field in order to characterize the resulting orientation estimation errors [21]. The second set of experiments involve exposing a triad of magnetometers to magnetic fields generated by various electrical appliances and ferrous objects in order to examine the magnitude of the errors and the range at which they occur. In the last set of experiments, a robot arm is tracked using inertial/magnetic sensor modules and an optical tracking system.

Errors Caused by Change in Magnetic Field Direction

In the first series of experiments, magnetic field variations were applied to the three types of sensor modules to measure the deviation in their orientation estimates due to the change in the sensed magnetic field. The change was generated using a Helmholtz coil. The sensors were placed inside the coil to observe how the orientation estimate would change as changes to the local direction of the local magnetic field were applied. The three different sensor modules tested were the MARG III, the MicroStrain 3DM-G, and the InterSense InertiaCube2.

Initial calibration data for the Helmholtz coil was obtained by applying different currents to it and measuring the induced field with a Hall probe. This initial data allowed decisions to be made regarding how much current was necessary to produce the desired magnetic inductions to be applied to the three different inertial/magnetic sensors. The selected magnetic field level was chosen to be on the order of the Earth's main field. The voltage that was necessary to reach the required magnetic induction was calculated using linear least square fit.

During the experiments, the Helmholtz coil was positioned to attempt to generate a magnetic induction that would be reversed approximately 180° in azimuth from the Earth's magnetic field. In most cases, the actual measured change ranged between 160° and 180° due to imprecise alignment of the coil relative to the local magnetic field vector. Each sensor module was placed in eight different orientations within the field generated by the Helmholtz coil. For each of the orientations the coil was energized to observe the type and magnitude of change that occurred in the orientation estimate produced by the sensor and its associated filtering algorithm [21].

The data plots from these experiments show a period of measuring the Earth's ambient magnetic field, followed by a period in which the Helmholtz coil was energized for 20 to 30 seconds. Following the energized period, the coil was de-energized and the plots reflect the return to sensing only the ambient field of the laboratory. The change in the direction and magnitude of the magnetic field vector is depicted in Figure 3. Energizing the coil caused the azimuth direction of the magnetic field vector to change from 0° to 180°. There was no significant change in the y (East) component of the vector. Since the coil was level, the z component of the magnetic field vector also remained unchanged. Prior to energizing of the coil, the magnetic field vector pointed North with a dip angle below the horizontal of 76°. While the coil was energized, the magnetic field vector pointed South with a negative elevation angle of 32°. Thus, in this series of experiments, not only were the sensor modules exposed to a full reversal of the azimuth direction of the magnetic field vector. Depending on their initial orientation relative to the magnetic field, the sensor modules were also exposed to a change in pitch, roll, or some combination of the two, totaling approximately 44°.

For visualization purposes, all orientation estimates produced by the sensors are displayed in Euler angle form. In the experiments presented here, the sensor modules were oriented in a North-East-Down reference orientation with the x axis of the module pointing towards the local North, the y axis

pointing East, and the z axis pointing down. At no time was a sensor actually rotated before, during, or after the application of the altered magnetic field.

Figure 4 and Figure 5 show the responses for the MARG III and MicroStrain 3DM-G, respectively, when the magnetic field was altered using the Helmholtz coil. In Figure 4, the MARG III was placed within the Hemholtz coil with an initial orientation of 2° roll, 10° yaw, and 3° pitch. Calibration of the MARG III does not account for nonorthogonality within the magnetometer triad. Thus, small changes and hysteresis can be seen in the roll and pitch estimates and the yaw estimate changes by an amount that is slightly less than the change in azimuth that occurred in the direction of the magnetic field. The smooth response of the MARG III filtering algorithm is due to the particular gain values used in the experiment. In Figure 5, the MicroStrain 3DM-G had an initial orientation of 2° roll, 13° yaw, and 0° pitch. Energizing the coil caused a 165° change in the yaw estimate produced by the sensor module. This change was equal in magnitude to the measured change in azimuth. No significant changes were observed in the roll and pitch estimates. The tuning of the orientation estimation algorithm provides an extremely sharp response to the change in the magnetic field direction. Both the MARG and MicroStrain sensors responded to the change in the sensed magnetic field by altering the yaw portion of their orientation estimates by an amount that was equal to measured azimuth change produced by the Helmholtz coil. Neither showed significant change in their roll and pitch estimates despite the fact that the direction of the magnetic field had changed both pitch angle and azimuth angle as depicted in Figure 3. This was true regardless of the orientation of the sensor modules relative to the coil. This is significant since it indicates the errors due to magnetic variation are restricted only to the horizontal plane. The estimates of pitch and roll are not affected by changes in the magnetic field direction for the sensors and algorithms tested [21]. This is in contrast to some

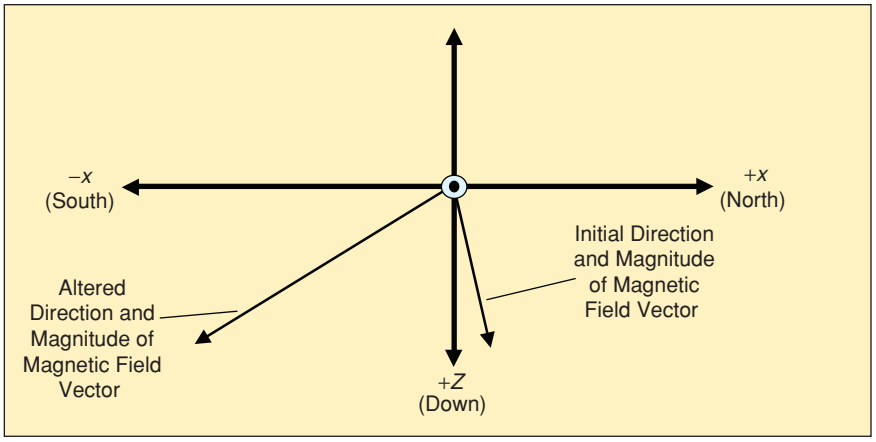

Figure 3. *Depiction of total change in the direction and magnitude of the magnetic field vector (East is directly out of the page).*

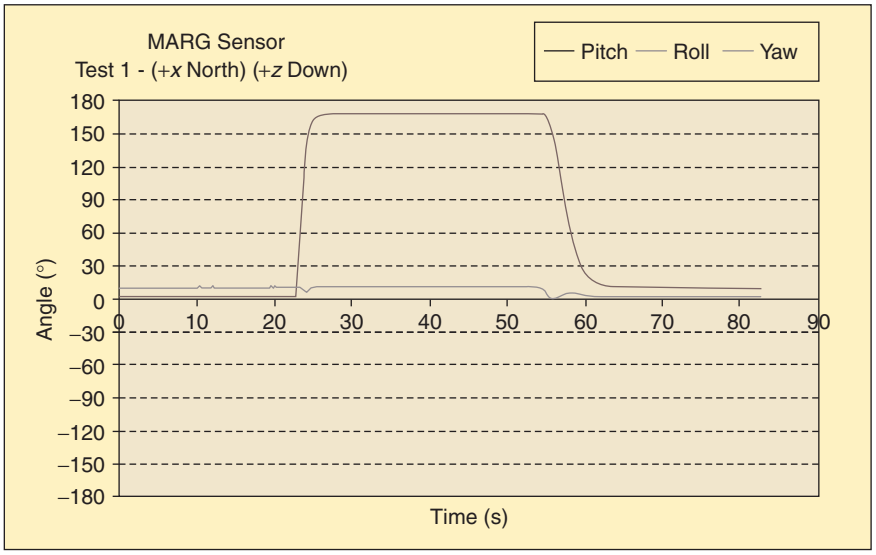

Figure 4. *MARG III sensor response to 180° azimuth change in the magnetic field direction.*

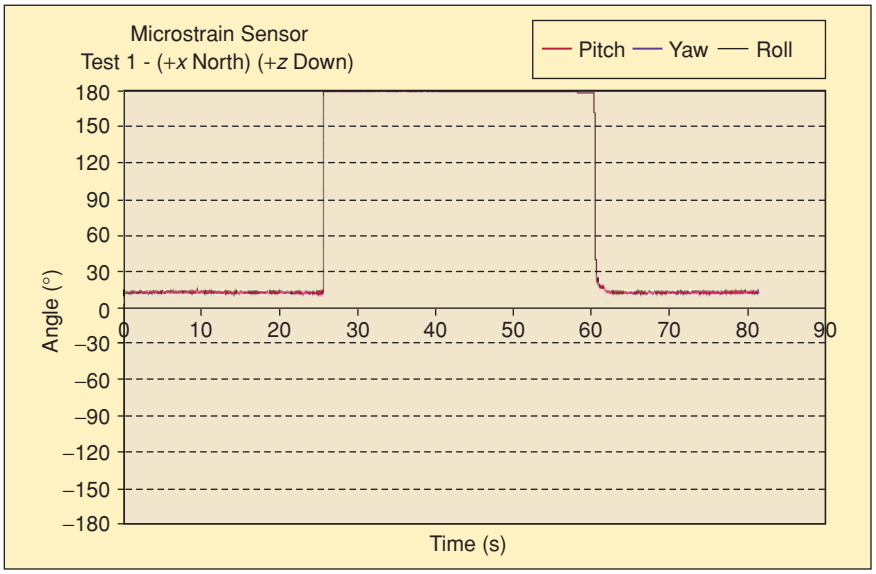

Figure 5. *MicroStrain 3DM-G response to 180° azimuth change in the magnetic field direction.*

orientation algorithms such as the QUEST [14], where such a change in the direction of the magnetic field will cause an error in both azimuth and pitch.

Figure 6 shows the response of the InertiaCube2 to the same magnetic variations as used in the experiments depicted in Figure 4 and Figure 5. Like the other sensors the orientation estimate changes only in azimuth. However, examination of Figure 6 indicates that unlike the other sensors, the estimated orientation produced by the InertiaCube2 algorithm changed by approximately 90° instead of 180°.

In order to investigate the response of the InertiaCube2 further, additional experiments were performed. In Figure 7, the sensor was again left in the same position within the Helmholtz coil. The coil was energized for approximately 30 seconds. Unlike previous experiments, during the time when the magnetic field was changing the sensor was physically tapped. This caused the estimated azimuth to proceed through a change that is similar to that observed with the other two sensor modules. Euler angle azimuth is bounded between 180° and -180°. Though the change is expressed as -180°, it is equivalent to the positive 180° change seen with the other two sensor modules. The knee seen in the trailing edge of Figure 7 is most likely the result of nonzero angular rate readings caused by tapping of the sensor module while the coil was being de-energized. These results indicate that the filtering algorithm of the InetiaCube2 will not accept changes in its orientation estimate without some accompanying nonzero reading from the angular rate sensors.

Based on the results of experiments described above, it appears that unlike active magnetic trackers that suffer estimation errors in all dimensions due to magnetic variations [22], variations in the direction of the local magnetic field only cause estimation errors in azimuth or the horizontal plan. The magnitude of the errors appears to be equal to the amount of deviation of the local magnetic field in the horizontal plane. No significant change was observed in the pitch and roll estimates produced by the three tested algorithms. These experimental results indicate that the dip angle itself or changes in the dip angle of the local magnetic field vector have no bearing on the accuracy or amount of variation seen in orientation estimates produced using inertial/magnetic sensor module data.

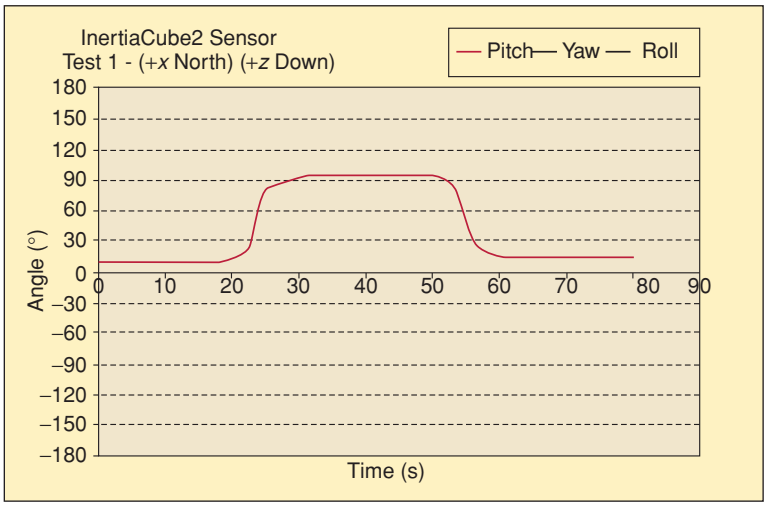

Figure 6. *Undisturbed InertiaCube 2 response to 180° change in the magnetic field direction.*

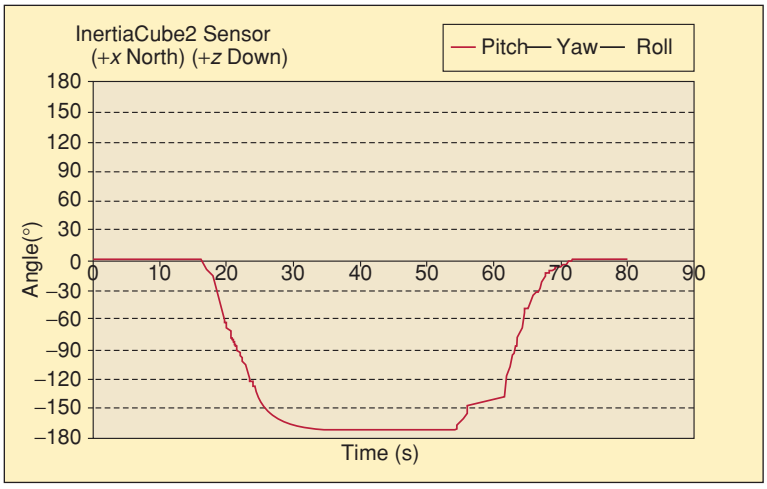

Figure 7. *Disturbed InertiaCube 2 response to 180° change in the magnetic field direction.*

Variations Caused by Common Objects

To determine the magnitude of azimuth errors that can be expected in a typical indoor environment, two types of experiments were performed. Initial experiments measured the magnetic field variation experienced at varying distances from several test objects. Later experiments measured the change in direction of the magnetic field vector at several positions in a magnetically noisy laboratory. The MARG III filtering algorithm utilizes a normalized magnetic field vector of unit length and is thus not affected by changes in the length of the magnetic field vector [3]. Based on manufacturer's literature, the algorithms associated with the InertiaCube and 3DM-G are similar in this regard. Therefore, the experimental results presented here concentrate on the changes in the direction of the local magnetic field and not changes in magnitude. The experiments described above establish that changes in the direction of the magnetic field orientation result only in azimuth errors for the orientation estimation algorithms associated with the tested sensor modules. Therefore, in the experiments described in this section, only magnetic deviation in the horizontal plane is examined.

To measure the magnetic deviation in the horizontal plane caused by test objects, a track was constructed using nonferrous materials and set so that the orientation of an inertial/magnetic sensor module could be held constant as the sensor was moved through successive positions approaching each object. The sensor module was placed at 18

locations with each successive location being 10 cm closer to the test object. In the final position the sensor module was within 1 cm of the test object. This set-up allowed the direction of the magnetic field vector to be measured since the sensor module orientation was kept constant. The test objects included:

- computer monitor (CRT type), powered and unpowered states
- simple appliance (small space heater with fan), powered and unpowered states
- electrical power supply, powered and unpowered states
- metal filing cabinet
- mobile robot, unpowered, powered, and motor engaged.

The MicroStrain 3DM-G sensor module is factory calibrated and allows access to scaled sensor output from each of the nine sensors in the module. The magnetometer triad in the 3DM-G sensor was used to measure the magnetic field direction in these experiments.

Prior to examination of the deviations caused by the test objects, a baseline was established by measuring the change in magnetic field direction with no object present. In the baseline case, the direction of the magnetic field in the horizontal plane deviated less the 1.6° as the sensor module was moved a distance of 180 cm down the test track. This deviation is attributed to noise in the ambient magnetic field of the laboratory. Comparison of these baseline deviations for each sampling position to the deviations that occurred when each of the test objects was present allows a more thorough understanding of the effects each object has on the magnetic field. The baseline was sampled before and after the experiments were conducted. This action helped to insure that no significant changes had occurred in the ambient magnetic field of the laboratory during the course of the experiments.

Figure 8 contains two subplots of data from experiments in which a CRT computer monitor was the test object. In each subplot, baseline average deviations are displayed along with the average deviations that occurred when the monitor was present. The top subplot displays the average deviations that occurred when the monitor was unpowered. The bottom subplot displays the average deviations with the monitor turned on and connected to a PC. The error bars represent the standard deviation of the data obtained at each position. The magnetic field showed approximately the same amount of deflection whether the monitor was attached to a PC and powered up or turned off. The standard deviations in both experiments are small and can be attributed to measurement noise, indicating the deviation was a dc effect. Some impact from this appliance can be observed to almost 40 cm of separation distance. In both cases, the computer monitor causes a maximum average deflection of 10.5° in the magnetic field relative to the horizontal plane.

Figure 9 shows two subplots of data from experiments in which a portable heater was used as a test object. In the first experiment both the heater fan and heating elements were off. In the second experiment both the fan and the heating elements were on. Examination of the two subplots indicates that the average amount of magnetic field deviation is significantly greater when the heater is turned on and increases dramatically as the sensor is brought in close proximity to the appliance. The standard deviations of the data taken at each position also increase significantly as the sensor is brought

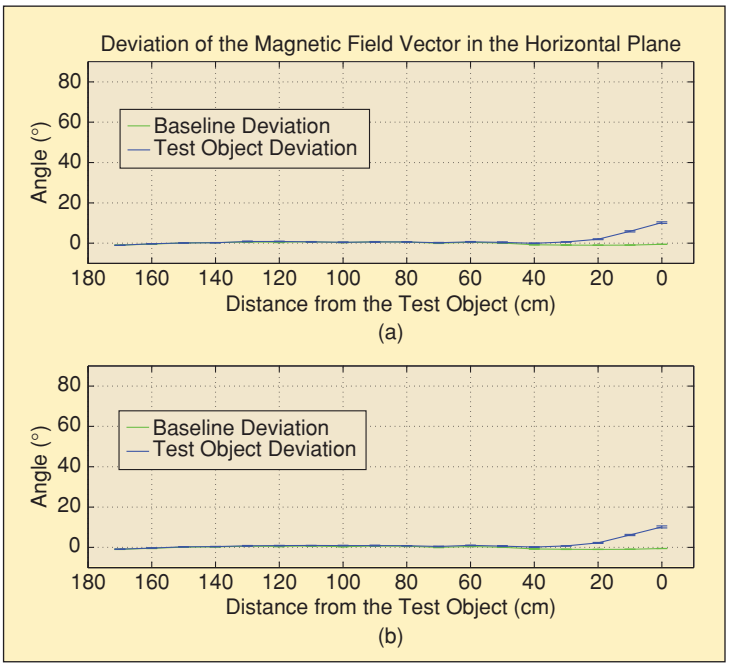

Figure 8. *Magnetic field vector deviation in the horizontal plane versus distance from a PC monitor in both (a) unpowered and (b) powered states.*

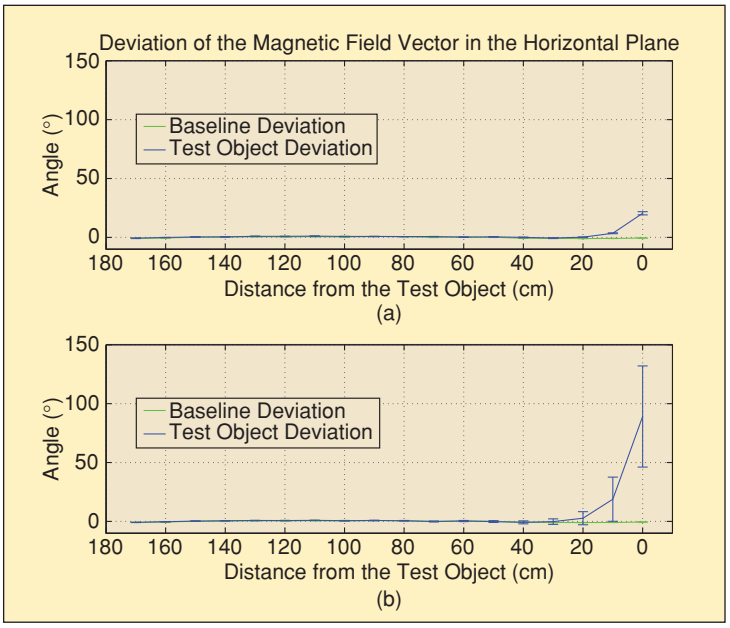

Figure 9. *Magnetic field vector deviation versus distance from an appliance (space heater) in both (a) unpowered and (b) powered states.*

closer to the running heater. This fluctuation is most likely due to the use of alternating current to power the appliance. With the heater in a powered-off state, the largest average deviation is 20.5°. With the heater turned on, the largest average deviation is nearly 90°. In both cases deviation caused by the heater did not begin to occur until the sensor module was within 30 cm of the heater.

Figure 10 shows two subplots of data from experiments in which an electrical power supply was used as a test object. In the first experiment the power supply is off. In the second experiment it is turned on and supplying power. The two subplots are very similar. The standard deviations of the data taken at each position are relatively small again indicating the deviation is dc in nature. In both subplots, the maximum average deviation is between 60° and 70°. The deviation due to the presence of the power supply begins to occur at a distance of nearly 1 m.

Figure 11 presents the deviation in the sensed magnetic field vector as the magnetometer triad of the sensor module approached a large metal filing cabinet. The deviations for this test object are the largest of any observed in the experiments described in this article. Large standard deviations for the data samples for each of the positions are not observed, indicating

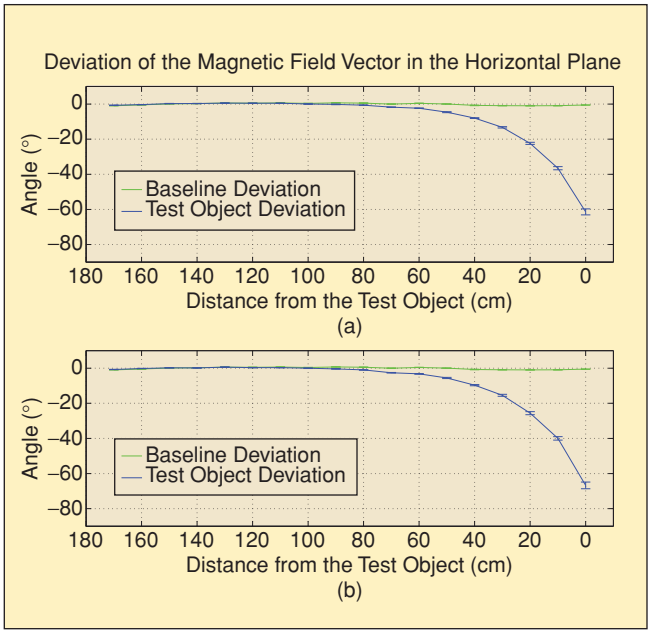

Figure 10. *Magnetic field vector deviation versus distance from an electrical power supply in both (a) unpowered and (b) powered states.*

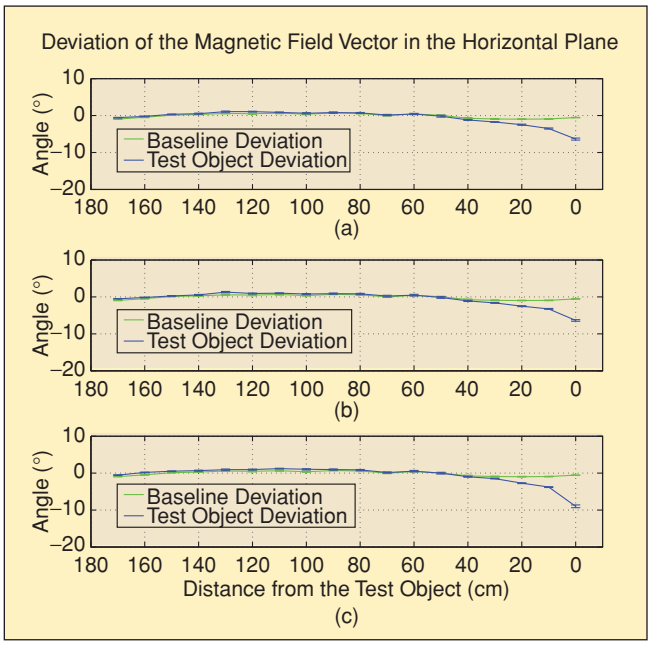

Figure 12. *Magnetic field vector deviation versus distance from a mobile robot in (a) motor-engaged, (b) systems-on, and (c) power-off states.*

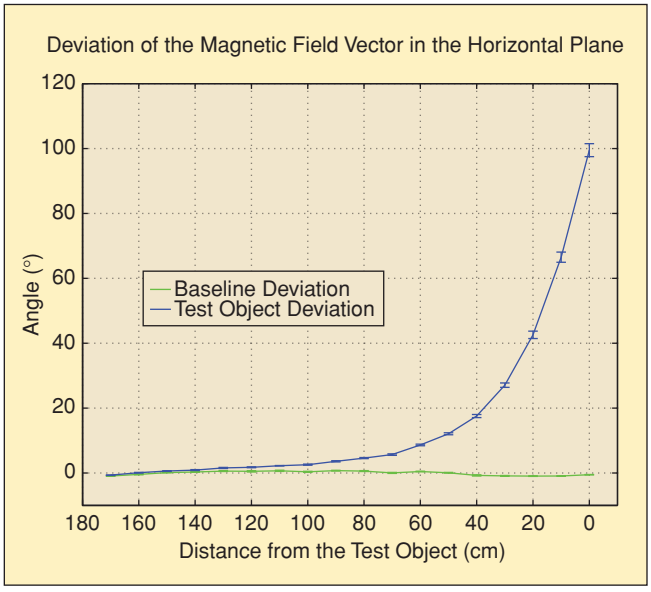

Figure 11. *Magnetic field vector deviation versus distance from a metal filing cabinet.*

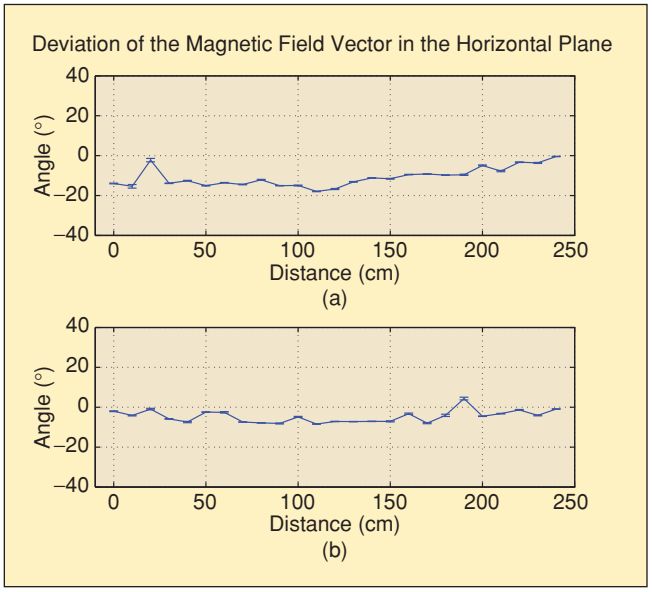

Figure 13. *Ambient magnetic field azimuth direction sampled at 10 cm intervals in a laboratory.*

that the magnetic field deviation was constant in nature. The maximum deflection caused by the filing cabinet is 99.5° and begins at a distance of 1.5 m.

The final test object presented is a Nomad Scout mobile robot. Magnetic deviation due to the presence of the robot was examined with the robot in three different states. These three states correspond to the three subplots in Figure 12. The bottom subplot displays the deviation induced by the robot when it is in an unpowered state. In the middle subplot, all electronic systems of the mobile robot were energized with the exception of the motor used to move the robot. The data displayed in the top subplot were collected while all robot systems were powered and the motors were engaged. The robot was placed on a stand so that its wheels could rotate freely. The maximum amount of average deviation observed for the robot is about 9°. This includes the case in which the motors were engaged. The standard deviation of the data for each position is relatively small. No deviation is observed beyond a distance of 40 cm.

Another set of experiments was conducted to examine the amount of variation that can be expected to occur in a laboratory environment in which numerous sources of magnetic noise are present. In these experiments, the azimuth direction of the magnetic field was measured at 25 positions at 10 cm intervals along a straight line with the sensor module orientation being held constant. As the sensor module being used to collect measurement data was moved it came within close proximity to numerous pieces of lab equipment simultaneously. The equipment included computer monitors, printers, mobile robots, servo control stations, and other miscellaneous lab equipment. Figure 13 contains subplots for two straight line samples. In the upper subplot, the azimuth direction of the magnetic field varies approximately 16°, with the maximum change between two adjacent positions being 13.1°. In the lower subplot, the azimuth direction of the magnetic field varies slightly less than 13°. The average difference from position to position is less than 3° for both trials. The accruing difference in the magnetic azimuth direction seen in the upper plot indicates the presence of a large-scale magnetic disturbance in the lab.

Overall, experiments in which the magnetic field variation caused by individual test objects was examined indicate that when inertial/magnetic sensor modules are separated by a distance of 1 m or more from most common appliances and ferrous objects the amount of azimuth error induced by those objects will be negligible. The amount of variation caused by different types of objects can vary significantly. The experimental results demonstrate that while inclination estimates can be expected to remain valid in close proximity to objects causing distortions in the local magnetic field, in some cases the azimuth estimates produced by the implemented algorithms had very little relation to the true orientation of the sensor module and can vary by as much as 100°. In other tests, azimuth estimates varied less than 10°. Experiments in which sensor modules were exposed to multiple sources of distortion simultaneously in a crowded laboratory environment show that azimuth estimates produced using a sensor module with a constant orientation can be significantly different for closely spaced positions. However, on average, differences in estimated azimuth from one position to another nearby position are much smaller.

Tracking a Robot Arm

The final experiments described in this article are designed to determine if inertial/magnetic sensor modules can be used to accurately track the orientation of the links of a robot arm made of ferrous materials. In these experiments a SCORBOT-ER III robot arm and three MicroStrain 3DM-G were utilized. The experiments concerning magnetic effects discussed above established that the response of the three different sensor modules to magnetic variations is essentially the same. In these tracking experiments, one 3DMG was securely attached to each link of the arm. While robot encoders provide incremental joint angle readings, use of these angles to obtain orientation estimates relative to an Earth-fixed reference frame requires forward kinematics and calibration, and the accuracy of the orientation estimates cannot be ascertained for this robot arm. As a result, the arm was also tracked using a Qualysis optical tracking system as depicted in Figure 14. The Qualysis system can be used to perform passive optical three degree-of-freedom position tracking and six degree-of-freedom tracking of designated rigid bodies on which four passive markers are mounted. Manufacturer's literature states that position accuracy is 0.1% of the field of view. The robot arm was contained in a 1-m^3 tracking volume. The Qualysis system utilized seven proflex cameras positioned around the

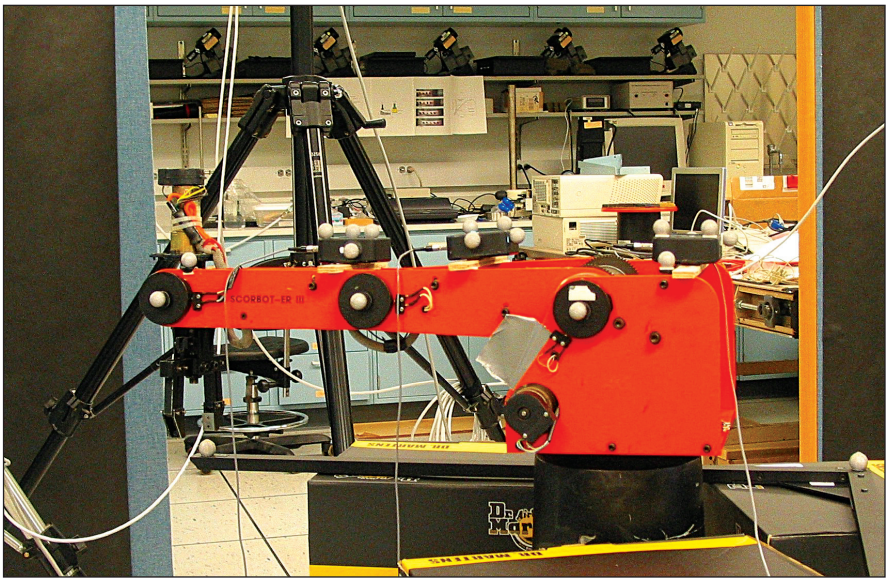

Figure 14. *SCORBOT-ER III robot arm instrumented for tracking with both inertial/magnetic sensor modules and an optical tracking system.*

tracking volume. In the experiments discussed here, 17 passive markers were used to track the position of the outboard end of each link and the orientation of the inertial/magnetic sensor module attached to each link. Each link was defined as a rigid body by placing four markers on the surface of the attached inertial/magnetic sensor. The geometric center of these four markers served as the origin of the local coordinate system of each segment. Following calibration, maximum residual error for all cameras was less than 1.127 mm. These calibration results indicate that the system was tracking to 1-mm accuracy as would be expected given the size of the tracking volume. Update rate for the optical tracking system was 60 Hz. Given this accuracy, data produced by this system were treated as a reference in these experiments.

Figure 15 shows a comparison of the orientation estimates produced using an inertial/magnetic sensor module and an optical tracking system while simultaneously tracking the robot arm. During the experiment, the robot arm was programmed to repeatedly trace an inclined square pattern with its end effecter. Due to a limited number of degrees of freedom in the arm, the programmed pattern did not require any of the tracked arm segments to roll. In Figure 15, yaw and pitch are shown for the most outboard end inertial/magnetic sensor. Examination of the Figure 15 shows that both tracking technologies produced very similar motion plots. Maximum steady-state difference between the orientation estimates produced using inertial/magnetic sensors and optical tracking is less than 2.5° in both subplots. This accuracy was achieved by the inertial/magnetic sensors despite the largely ferrous nature of the material of which the robot arm was constructed and the presence and operation of several servo motors used to position and move the arm.

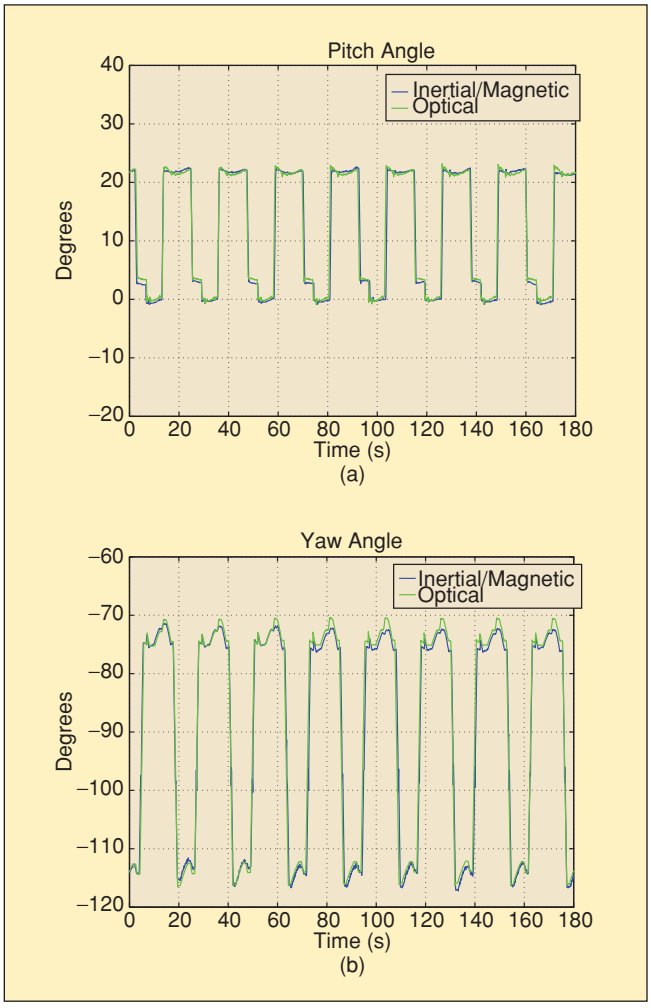

Figure 15. *Comparison of yaw and pitch orientation estimates for a robot arm segment produced by an optical tracking system and an inertial/magnetic sensor module.*

Conclusions and Discussion

The direction of the local magnetic field vector can be altered by the presence of operating electrical appliances or objects made of ferrous materials. The assumption made by orientation estimation algorithms that the direction of the local magnetic field is static makes the algorithms susceptible to errors as the sensor modules are moved from one position to another within a tracking volume. In the algorithms tested, the errors appear only in the azimuth portions of the orientation estimates produced. These errors will be roughly equal in size to the amount the magnetic field deviates in the horizontal plane from the original reference.

The amount of deviation caused by appliances and ferrous objects can range from very small to very large. The horizontal deviation of the magnetic field was measured for several common objects. Maximum deviation ranged from 10.5° to nearly 100°. Experimental data presented here indicate that such deviations can be largely avoided by maintaining a distance of approximately 1 m from the source of interference. Only one of the objects caused a horizontal plane deviation at a distance of more than one meter. For this object, horizontal plan deviations did not exceed 4° when at a distance of more than 1 m. For many of the objects, no deviation was observed beyond a distance of a half meter. However, in an indoor environment containing numerous sources of interference, it can be difficult to determine which objects are the major contributors to magnetic field deflections and the magnetic field can vary significantly between closely spaced positions.

Despite all the above, the tracking experiments indicate that inertial/magnetic sensor modules can be used to track posture with an accuracy that is comparable to optical tracking. The accuracy of the orientation estimates while tracking a robot arm using data from inertial/magnetic sensor modules indicates that such modules can be used to accurately track orientation in environments and applications in which operating motors and ferrous objects are present. However, given the current state of the art of orientation estimation algorithms designed to process inertial/magnetic sensor module data, they should not be used in an application without first investigating the nature of the magnetic field in the environment in which they will utilized. While Rotenberg et al. have begun the investigation of modified algorithms designed to alleviate the effects of magnetic variations in [23], further work is needed. This work should include an investigation of the use of arrays of sensor modules placed at slightly different positions and a method of estimating the relative amount of interference to which each individual module is exposed.

Acknowledgments

This work was in part supported by the Army Research Office (ARO project number 40410-MA) and the U.S. Navy Modeling and Simulation Office (NMSO). The authors would like to thank the National Institute of Occupational Safety and Health (NIOSH) for allowing the use of their equipment and laboratory facilities for the collection of portions of the experimental data presented. The findings and conclusions in this report are those of the authors and do not necessarily represent the views of NIOSH.

Keywords

Motion measurement, inertial sensors, orientation estimation, magnetic fields, accelerometers, magnetometers, optical tracking.

References

[1] G. Dissanayake, S. Sukkarieh, E. Nebot, and H. Durant-Whyte, "The aiding of a low-cost strapdown inertial measurement unit using vehicle model constraints for land vehicle applications," *IEEE Trans. Robot. Automat.*, vol. 17, pp. 731–747, Oct. 2001.

[2] S. Sarapalli, J. Roberts, P. Corke, G. Buskey, and G. Sukhatme, "A tale of two helicopters," in *Proc. 2003 IEEE/RSJ Int. Conf. Intelligent Robots and Systems*, Las Vegas, NV, pp. 805–810, Oct. 2003.

[3] E. Bachmann, R. McGhee, X. Yun, and M. Zyda, "Inertial and magnetic posture tracking for inserting humans into networked virtual environments," in *Proc. ACM Symp. Virtual Reality Software and Technology (VRST) 2001*, Banff, Canada, pp. 9–16, Nov. 2001.

[4] K. Meyer, H. Applewhite, and F. Biocca, "A survey of position trackers," *Presence: Teleoperators and Virtual Environments*, vol. 1, no. 2, pp. 173–200, 1992.

[5] E. Foxlin, M. Harrington, and Y. Alshuler, "Miniature 6-DOF inertial system for tracking HMDs," *SPIE, Helmet and Head-Mounted Displays III*, vol. 3362, Apr. 1998.

[6] E. Foxlin, "Inertial head-tracker fusion by a complementary separate-bias Kalman filter," in *Proc. Virtual Reality Annu. Int. Symp. (VRAIS 96)*, Santa Clara, CA, pp. 185–194, Mar. 1996.

[7] E. Bachmann, "Inertial and magnetic tracking of limb segment orientation for inserting humans into synthetic environments," Ph.D. dissertation, Naval Postgraduate School, Monterey, CA, 2000.

[8] A. Gallagher, Y. Matsuok, and A. Wei-Tech, "An efficient real-time human posture tracking algorithm using low-cost inertial and magnetic sensors," in *Proc. 2004 IEEE Int. Conf. Robotics and Automation*, Sendai, Japan, pp. 2967–2972, Sept. 2004.

[9] H.J. Luinge, "Inertial sensing of human movement," Ph.D. dissertation, University of Twente, Dec. 2002.

[10] R. Zhu and Z. Zhou, "A real-time articulated human motion tracking using tri-axis inertial/magnetic sensors package," *IEEE Trans. Neural Syst. Rehabil. Eng.*, vol. 12, pp. 295–302, June 2004.

[11] E. Kraft, "A quaternion-based unscented Kalman filter for orientation tracking," in *Proc. IEEE 6th Int. Conf. Information Fusion*, Cairns, Queensland, Australia, pp. 47–54, 2003.

[12] Z. Yan and K. Yuan, "An orientation tracking algorithm valid in a hemisphere space based on gravity field and earth magnetic field," in *Proc. 2004 IEEE Int. Conf. Information Acquisition*, Hefei, China, pp. 236–239, June 2004.

[13] D. Gebre-Egziabher, G.H. Klkaim, J. Powell, and B.W. Parkinson, "A gyro-free quaternion-based attitude determination system suitable for implementation using low cost sensors," in *Proc. IEEE 2000 Position Location and Navigation Symp.*, San Diego, CA, pp. 185–192, Mar. 2000.

[14] M.D. Shuster and S.D. Oh, "Three-axis attitude determination for vector observations," *J. Guidance Control*, vol. 4, no. 1, pp. 70–77, 1981.

[15] E. Bachmann, X. Yun, D. McKinney, R. McGhee, and M. Zyda, "Design and implementation of MARG sensors for 3-DOF orientation measurement of rigid bodies," in *Proc. IEEE Int. Conf. Robotics and Automation (ICRA 2003)*, Taipei, Taiwan, pp. 1171–1178, Sept. 2003.

[16] X. Yun, C. Aparicio, E. Bachmann, and R. McGhee, "Implementation and experimental results of a quaternion-based Kalman filter for human body motion tracking," in *Proc. 2005 IEEE Int. Conf. Robotics and Automation*, Barcelona, Spain, pp. 317–322, Apr. 2005.

[17] W. Denne, *Magnetic Compass Deviation and Correction*, 3rd Ed. Glasgow: Brown and Ferguson, 1979.

[18] T.S. Tenforde, "Spectrum and intensity of environmental electromagnetic fields from natural and man-made sources," in *Electromagnetic Fields: Biological Interactions and Mechanisms*, Washington, DC: American Chemical Society, pp. 13–35, 1995.

[19] M. Caruso, "Applications of magnetic sensors for low cost compass systems," in *Proc. IEEE Symp. Position Location and Navigation*, San Diego, CA, pp. 177–184, Mar. 2000.

[20] B. Hoff, and R. Azuma, "Autocalibration of an electronic compass in an outdoor reality system," in *Proc. IEEE Symp. Augmented Reality (ISAR 2000)*, Munich, Germany, pp. 159–164, Oct. 2000.

[21] C. Peterson, "An investigation of the effects of magnetic variations on inertial/magnetic orientation sensors," Master's thesis, Miami University, Oxford, OH., 2003.

[22] M. Nixon, B. McCallum, W. Fright, and N. Price, "The effects of metals and interfering fields on electromagnetic trackers," *Presence: Teleoperators and Virtual Environments*, vol. 7, no. 2, pp. 204–218, 1998.

[23] D. Roetenberg, H.J. Luinge, C.T.M. Baten, and P.H. Veltink, "Compensation of magnetic disturbances improves inertial and magnetic sensing of human body segment orientation," *IEEE Trans. Neural Syst. Rehabil. Eng.,* vol. 13, pp. 395–405, Sept. 2005.

Eric R. Bachmann holds positions as an associate professor at Miami University in Oxford, Ohio, and as a research assistant professor at the Naval Postgraduate School in Monterey, California. Prior to this he served as an officer and an unrestricted naval aviator in the U.S. Navy. His research interests include virtual environments, computer graphics, and visualization. He holds a bachelor's degree from the University of Cincinnati and M.S. and Ph.D. degrees from the Naval Postgraduate School. He is a member of IEEE.

Xiaoping Yun is a professor of electrical and computer engineering at the Naval Postgraduate School in Monterey, California. His research interests include coordinated control of multiple robotic manipulators, mobile manipulators, mobile robots, control of nonholonomic systems, MEMS sensors, carbon nanotubes-based sensors, and inertial/magnetic human body motion tracking. He holds a B.S from Northeastern University, China, and M.S. and Ph.D. degrees from Washington University in St. Louis, Missouri. He is currently treasurer of the IEEE Robotics and Automation Society and vice president for finance of the IEEE Nanotechnology Council. He is a Fellow of IEEE.

Anne Brumfield has worked in the Engineering and Control Technology Branch at the National Institute of Occupational Safety and Health since 2001 in the field of sensors and instrumentation.

***Address for Correspondence*:** Eric R. Bachmann, Kreger 217D, Department of Computer Science and Systems Analysis, Miami University, Oxford, OH 45056. Phone: +1 513 529 1239. Fax: +1 513 529 1524. E-mail: bachmaer@muohio. edu.